Inorg. Chem. **2007**, *46*, 3669–3679

Probing Anion–π Interactions in 1-D Co(II), Ni(II), and Cd(II) Coordination Polymers Containing Flexible Pyrazine Ligands

Cory A. Black,[†] Lyall R. Hanton,*[,†] and Mark D. Spicer[‡]

Department of Chemistry, University of Otago, P.O. Box 56, Dunedin, New Zealand, and WestCHEM, Department of Pure and Applied Chemistry, University of Strathclyde, 295 Cathedral Street, Glasgow G1 1XL, Scotland

Received February 1, 2007

Two flexible thioether-containing heterocyclic ligands bis(2-pyrazylmethyl)sulfide (**L1**) and 2-benzylsulfanylmethylpyrazine (**L2**) have arene rings with differing π-acidities which were used to probe anion–π binding in five 1-D coordination polymers formed from the metal salts $Co(ClO_4)_2$, $Ni(NO_3)_2$, and $Cd(NO_3)_2$. In $\{[Co(\mathbf{L1})(MeCN)_2](ClO_4)_2\}_\infty$ (**1**), $\{[Ni(\mathbf{L1})(NO_3)_2]\}_\infty$ (**2**), and $\{[Cd_2(\mathbf{L1})(MeCN)(H_2O)(NO_3)_4]\cdot H_2O\}_\infty$ (**3·H₂O**), the symmetrical ligand **L1** was bound facially to the metal center and was bridged through a pyrazine donor to an adjacent metal forming a polymer chain. The folding of **L1** formed U-shaped π-pockets in **1** and **3·H₂O** which encapsulated free and bound anions, respectively. The anions interacted with the π-acidic centers in a variety of different binding modes including anion–π–anion and π–anion–π sandwiching. A wider π-pocket was formed in **2** which also contained anion–π interactions. The polymer chains in **2** were interdigitated through a rare type of complementary T-shaped N(pyrazine)$\cdots\pi$ interaction. In $\{[Co(\mathbf{L2})(H_2O)_3](ClO_4)_2\cdot H_2O\}_\infty$ (**4·H₂O**) and $\{[Cd(\mathbf{L2})(H_2O)(NO_3)_2]\}_\infty$ (**5**), the unsymmetrical ligand **L2** chelated the metal center and bridged through a pyrazine donor to an adjacent metal forming a polymer chain. The ligand arrangement resulted in the anions in both structures being involved in only anion–π–anion sandwich interactions. In **4·H₂O**, the noncoordinated ClO_4^- anions interacted with only one chain while in **5** the coordinated NO_3^- anions acted as anion–π supramolecular synthons between chains. Comparison between the polymers formed with ligands **L1** and **L2** showed that only the more π-acidic ring was involved in the anion–π interactions.

Introduction

Anion−host interactions are important in a variety of systems including those involving anion interactions with natural−biological[1] or synthetic−inorganic[2] receptors.[3] Whether a host is cationic or neutral, an anion can be expected to experience an electrostatic interaction with the host because of charge differences. These electrostatic interactions are nondirectional, and as a result, the whole host is a binding site, although some sites will interact more strongly than others. However, intuitively anions are not expected to interact with neutral aromatic π clouds because any interaction between the two should be repulsive.[4] It is only recently through the investigations of π-acidic systems that anion−π interactions have begun to receive any attention. Extensive calculations have confirmed that π-acidic systems as diverse as halo-,[5−8] nitro-, and cyano-substituted benzenes,[9] halo-[8] and cyano-ethenes,[9] cyanuric acids,[10] cyclopentadiene derivatives,[11] tetrazines,[12] and triazines[4,6−8,10a,13,14] can interact with simple anions such as halides or multiatomic anions such as NO_3^- and BF_4^-. Recently MeCN has

* To whom correspondence should be addressed. Fax: (+64) 3-479-7906. Phone: (+64) 3-479-7918. E-mail: lhanton@alkali.otago.ac.nz.
[†] University of Otago.
[‡] University of Strathclyde.

(1) (a) Beer, P. D.; Gale, P. A. *Angew. Chem., Int. Ed.* **2001**, *40*, 486−516. (b) Gale, P. A. *Coord. Chem. Rev.* **2000**, *199*, 181−233. (c) Mangani, S.; Ferraroni, M. Natural Anion Receptors: Anion Recognition by Proteins. In *Supramolecular Chemistry of Anions*; Bianchi, A., Bowman-James, K., Garcia-España, E., Eds.; Wiley: New York, 1997; pp 63−78.
(2) (a) Amendola, V.; Bonizzoni, M.; Esteban-Gómez, D.; Fabbrizzi, L.; Licchelli, M.; Sancenón, F.; Taglietti, A. *Coord. Chem. Rev.* **2006**, *250*, 1451−1470. (b) Amendola, V.; Boiocchi, M.; Colasson, B.; Fabbrizzi, L. *Inorg. Chem.* **2006**, *45*, 6138−6147. (c) Vega, I. E. D.; Gale, P. A.; Light, M. E.; Loeb, S. J. *Chem. Commun.* **2005**, 4913−4915. (d) Bondy, C. R.; Gale, P. A.; Loeb, S. J. *J. Am. Chem. Soc.* **2004**, *126*, 5030−5031.
(3) (a) Gale, P. A. *Acc. Chem. Res.* **2006**, *39*, 465−475. (b) Yoon, J.; Kim, S. K.; Singh, N. J.; Kim, K. S. *Chem. Soc. Rev.* **2006**, *35*, 335−360. (c) Bowman-James, K. *Acc. Chem. Res.* **2005**, *38*, 671−678. (d) Bondy, C. R.; Loeb, S. J. *Coord. Chem. Rev.* **2003**, *240*, 77−99.
(4) Mascal, M.; Armstrong, A.; Bartberger, M. D. *J. Am. Chem. Soc.* **2002**, *124*, 6274−6276.

10.1021/ic070194k CCC: $37.00
Published on Web 03/16/2007

been shown to interact with a π-acidic tetrazine ligand in a $ZnCl_2$ complex.[15] One of the challenges in this area is to design appropriate chemical systems incorporating sufficient π-acidity. Metal−ligand interactions involving heterocyclic rings have potential in this area. The presence of the heteroatom perturbs the π-electron density of the ring which is further polarized upon coordination of a positively charged metal ion.[16] In most cases, simple metal complexes will not provide sufficient polarization to produce anion−π binding. However, when ligands incorporate heterocycles that have more than one donor in the ring, the potential for bridging between metal ions exists resulting in a more π-acidic heterocyclic ring center. These requirements are likely to be met for coordination polymers when the appropriate ligands are used. Coordination polymers have another advantage, as through design or packing, they often form cavities bounded by arene rings in which the anion may be situated.[17] In certain circumstances, these cavities are reminiscent of the π-acidic interiors of some molecular containers which are used as anion receptors.[18] Recently, additivity of anion−π interactions has been identified as a factor leading to increased anion binding energies.[13b] Frequently, pyridine-based ligands predominate in metallo−supramolecular systems, and so it has taken the introduction of ligands based on triazine[13a,19] and tetrazine[20] to draw attention to this weak interaction. Compounding this issue is the abundance of information

Chart 1

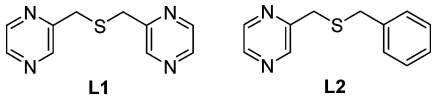

contained within crystal structures which has caused anion−π interactions to go unnoticed or overlooked for many years.[5d] As a consequence of the interest engendered by supramolecular chemistry which has encouraged the detailed analysis of crystal structures, the nature of weaker interactions has been studied and their importance identified.[16,21] Interactions which have been accepted into the supramolecular paradigm include weak hydrogen bonds such as C−H···O[22] and C−H···N[23] and N−H···Cl[21d,24] interactions.

We have designed two related flexible multimodal thioether ligands incorporating one or two pyrazine rings (Chart 1). Reaction of these ligands with selected d-block elements led to bridging of the pseudo-octahedral metal ions by a pyrazine ring resulting in the formation of 1-D coordination polymers. The metal−ion polarized pyrazine rings have a π-acidic center leading to a close association of anions. Recent calculations have shown that 2,5-dichloropyrazine[7] and tetracyanopyrazine[9] can interact favorably with halide

(5) (a) Garau, C.; Frontera, A.; Quiñonero, D.; Ballester, P.; Costa, A.; Deyà, P. M. *Chem. Phys. Lett.* **2004**, *392*, 85−89. (b) Garau, C.; Frontera, A.; Quiñonero, D.; Ballester, P.; Costa, A.; Deyà, P. M. *Chem. Phys. Lett.* **2004**, *399*, 220−225. (c) Alkorta, I.; Elguero, J. *J. Phys. Chem. A* **2003**, *107*, 9428−9433. (d) Quiñonero, D.; Garau, C.; Rotger, C.; Frontera, A.; Ballester, P.; Costa, A.; Deyà, P. M. *Angew. Chem., Int. Ed.* **2002**, *41*, 3389−3392.

(6) (a) Quiñonero, D.; Garau, C.; Frontera, A.; Ballester, P.; Costa, A.; Deyà, P. M. *J. Phys. Chem. A* **2005**, *109*, 4632−4637. (b) Garau, C.; Frontera, A.; Quiñonero, D.; Ballester, P.; Costa, A.; Deyà, P. M. *ChemPhysChem* **2003**, *4*, 1344−1348.

(7) Garau, C.; Frontera, A.; Quiñonero, D.; Ballester, P.; Costa, A.; Deyà, P. M. *J. Phys. Chem. A* **2004**, *108*, 9423−9427.

(8) Kim, D.; Tarakeshwar, P.; Kim, K. S. *J. Phys. Chem. A* **2004**, *108*, 1250−1258.

(9) Rosokha, Y. S.; Lindeman, S. V.; Rosokha, S. V.; Kochi, J. K. *Angew. Chem., Int. Ed.* **2004**, *43*, 4650−4652.

(10) (a) Mascal, M. *Angew. Chem., Int. Ed.* **2006**, *45*, 2890−2893. (b) Frontera, A.; Saczewski, F.; Gdaniec, M.; Dziemidowicz-Borys, E.; Kurland, A.; Deyà, P. M.; Quiñonero, D.; Garau, C. *Chem. Eur. J.* **2005**, *11*, 6560−6567.

(11) Garau, C.; Frontera, A.; Quiñonero, D.; Ballester, P.; Costa, A.; Deyà, P. M. *Chem. Phys. Lett.* **2003**, *382*, 534−540.

(12) (a) Schottel, B. L.; Chifotides, H. T.; Shatruk, M.; Chouai, A.; Pérez, L. M.; Bacsa, J.; Dunbar, K. R. *J. Am. Chem. Soc.* **2006**, *128*, 5895−5912. (b) Garau, C.; Quiñonero, D.; Frontera, A.; Costa, A.; Ballester, P.; Deyà, P. M. *Chem. Phys. Lett.* **2003**, *370*, 7−13.

(13) (a) Maheswari, P. U.; Modec, B.; Pevec, A.; Kozlevèar, B.; Massera, C.; Gamez, P.; Reedijk, J. *Inorg. Chem.* **2006**, *45*, 6637−6645. (b) Garau, C.; Quiñonero, D.; Frontera, A.; Ballester, P.; Costa, A.; Deyà, P. M. *J. Phys. Chem. A* **2005**, *109*, 9341−9345.

(14) Casellas, H.; Massera, C.; Buda, F.; Gamez, P.; Reedijk, J. *New J. Chem.* **2006**, *30*, 1561−1566.

(15) Mooibroek, T. J.; Teat, S. J.; Massera, C.; Gamez, P.; Reedijk, J. *Cryst. Growth Des.* **2006**, *6*, 1569−1574.

(16) Janiak, C. *J. Chem. Soc., Dalton Trans.* **2000**, 3885−3896.

(17) Gural'skiy, I. A.; Solntsev, P. V.; Krautscheid, H.; Domasevitch, K. V. *Chem. Commun.* **2006**, 4808−4810.

(18) For example: (a) Gamez, P.; Reedijk, J. *Eur. J. Inorg. Chem.* **2006**, 29−42. (b) Fairchild, R. M.; Holman, K. T. *J. Am. Chem. Soc.* **2005**, *127*, 16364−16365.

(19) (a) de Hoog, P.; Gamez, P.; Mutikainen, I.; Turpeinen, U.; Reedijk, J. *Angew. Chem., Int. Ed.* **2004**, *43*, 5815−5817. (b) Demeshko, S.; Dechert, S.; Meyer, F. *J. Am. Chem. Soc.* **2004**, *126*, 4508−4509.

(20) (a) Campos-Fernández, C. S.; Schottel, B. L.; Chifotides, H. T.; Bera, J. K.; Bacsa, J.; Koomen, J. M.; Russell, D. H.; Dunbar, K. R. *J. Am. Chem. Soc.* **2005**, *127*, 12909−12923. (b) Campos-Fernández, C. S.; Clérac, R.; Koomen, J. M.; Russell, D. H.; Dunbar, K. R. *J. Am. Chem. Soc.* **2001**, *123*, 773−774. (c) Campos-Fernández, C. S.; Clérac, R.; Dunbar, K. R. *Angew. Chem., Int. Ed.* **1999**, *38*, 3477−3479.

(21) (a) Umezawa, Y.; Tusboyama, S.; Honda, K.; Uzawa, J.; Nishio, M. *Bull. Chem. Soc. Jpn.* **1998**, *71*, 1207−1213. (b) Dance, I. *New J. Chem.* **2003**, *27*, 22−27. (c) Janiak, C.; Scharmann, T. G. *Polyhedron* **2003**, *22*, 1123−1133. (d) Lewis, G. R.; Orpen, A. G. *Chem. Commun.* **1998**, 1873−1874.

(22) (a) Desiraju, G. R. *Chem. Commun.* **2005**, 2995−3001. (b) Gu, Y.; Kar, T.; Scheiner, S. *J. Am. Chem. Soc.* **1999**, *121*, 9411−9422. (c) Desiraju, G. R. *Acc. Chem. Res.* **1996**, *29*, 441−449. (d) Steiner, T. *Cryst. Rev.* **1996**, *6*, 1−51.

(23) (a) Amoore, J. J. M.; Hanton, L. R.; Spicer, M. D. *Dalton Trans.* **2003**, 1056−1058. (b) Ohkita, M.; Kawano, M.; Suzuki, T.; Tsuji, T. *Chem. Commun.* **2002**, 3054−3055. (c) Thalladi, V. R.; Gehrke, A.; Boese, R. *New J. Chem.* **2000**, *24*, 463−470. (d) Cotton, F. A.; Daniels, L. M.; Jordan, G. T., IV; Murillo, C. A. *Chem. Commun.* **1997**, 1673−1674. (e) Mascal, M. *Chem. Commun.* **1998**, 303−304.

(24) (a) Adams, C. J.; Angeloni, A.; Orpen, A. G.; Podesta, T. J.; Shore, B. *Cryst. Growth Des.* **2006**, *6*, 411−422. (b) Custelcean, R.; Haverlock, T. J.; Moyer, B. A. *Inorg. Chem.* **2006**, *45*, 6446−6452. (c) Zhang, J.; Ye, L.; Wu, L. *J. Mol. Struct.* **2006**, *791*, 172−179. (d) Kumar, D. K.; Ballabh, A.; Jose, D. A.; Dastidar, P.; Das, A. *Cryst. Growth Des.* **2005**, *5*, 651−660.

(25) (a) Otwinowski, Z.; Minor, W. In *Processing of X-Ray Diffraction Data Collected in Oscillation Mode*; Carter, C. W., Jr., Sweet, R. M., Eds.; Methods in Enzymology, Vol. 276; Academic Press: New York, 1997; pp 307−326. (b) *SAINT V4, Area Detector Control and Integration Software*; Siemens Analytical X-Ray Systems Inc.: Madison, WI, 1996.

(26) Sheldrick, G. M. *SADABS, Program for Absorption Correction*; University of Göttingen: Göttingen, Germany, 1996.

(27) Sheldrick, G. M. *Acta Crystallogr., Sect. A* **1990**, *46*, 467−473.

(28) Altomare, A.; Burla, M. C.; Camalli, M.; Cascarano, G. L.; Giacovazzo, C.; Guagliardi, A.; Moliterni, A. G. G.; Polidori, G.; Spagna, R. *J. Appl. Cryst.* **1999**, *32*, 115−119.

(29) Sheldrick, G. M. *SHELXL-97, Program for the Solution of Crystal Structures*; University of Göttingen: Göttingen, Germany, 1997.

(30) Farrugia, L. J. *J. Appl. Crystallogr.* **1999**, *32*, 837−838.

(31) Spek, A. L. *Acta Crystallogr., Sect. A* **1990**, *46*, C34.

(32) (a) Macrae, C. F.; Edgington, P. R.; McCabe, P.; Pidcock, E.; Shields, G. P.; Taylor, R.; Towler, M.; van de Streek, J. *J. Appl. Cryst.* **2006**, *39*, 453−457. (b) Bruno, I. J.; Cole, J. C.; Edgington, P. R.; Kessler, M. K.; Macrae, C. F.; McCabe, P.; Pearson, J.; Taylor, R. *Acta Crystallogr., Sect. B* **2002**, *58*, 389−397.

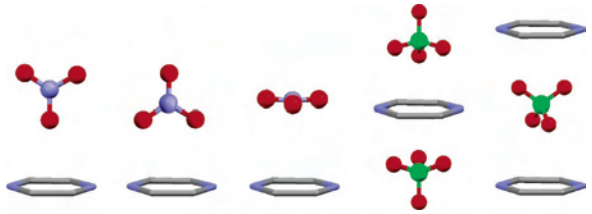

Figure 1. Examples of the different types of anion−π interaction observed for polymers **1**−**5** (left to right), one donor, two donor, planar arrangement, anion− π−anion, and π−anion−π.

anions. This interaction between an anion and a π system is observed in our work with both free (ClO_4^-) and bound (NO_3^-) anions. Significantly, this means that the anion−π interactions we have identified occur with both cationic and neutral 1-D coordination polymer chains. The ligands **L1** and **L2** were used to test the affinity of multiatomic anions toward coordinated pyrazine rings. Multiatomic anions have been less well studied perhaps because they are bulkier and have a more dispersed charge.[12a] The symmetric ligand **L1** has two pyrazine rings both capable of participating in anion−π interactions. The unsymmetric ligand **L2** has one pyrazine and one benzene ring which present the anions with different π acidities providing an ability to tune the structural outcome. In our systems, the anion−π interactions on average are found to be weaker than those observed in metal triazine[13a,19] or tetrazine[12a,20] systems which have more heteroatoms in the rings. The influence of the number of heteroatoms in a ring has previously been examined in a comparative study using Ag(I) complexes of the related ligands 3,6-bis(2′-pyridyl)-1,2,4,5-tetrazine and 3,6-bis(2′-pyridyl)-1,2-pyridazine.[12a] The study shows that the less π-acidic pyridazine systems have weaker anion−π interactions than the analogous tetrazine systems. However, this can be compensated for by the additivity of these interactions.[13b] Indeed, we have found that it is possible to achieve multiple anion−π interactions by using a flexible pyrazine ligand which is incorporated into a coordination polymer. We observed various different types of anion−π arrangements, many of them presaged in theoretical calculations (Figure 1).[5d,8] Our structures included anions interacting through one or two donor atoms and in a planar fashion. Four of the polymers also displayed unusual anion−π−anion or π−anion−π sandwich-type interactions.[13] Remarkably, two of the structures involving different anions displayed both types of sandwiching.

Experimental Section

General. The ligand bis(2-pyrazylmethyl)sulfide (**L1**) was prepared via literature methods.[33] Infrared spectra were measured on a Perkin−Elmer Win−IR Spectrum BX FT−IR System (samples in KBr disks). Elemental analyses were performed by the Campbell Microanalytical Laboratory at the University of Otago. Samples were predried under vacuum to remove volatile solvent residues. The solid-state electronic spectra were collected as a $BaSO_4$ diluted sample with a Cary−500 Scan UV−vis−NIR spectrophotometer fitted with a 110-mm PTFE coated integrating sphere. The electrospray mass spectrum (ES−MS) was measured on a Shimadazu LCMS−QP800α spectrometer with a mass range *m*/*z* 10−1000. Samples were injected by direct infusion using a Rheodyne manual injector. The mobile phase flow rate was 0.2 mL min^{-1} using MeCN as solvent.

Caution: Although no problems were encountered in this work, transition-metal perchlorates are potentially explosive. They should be prepared in small amounts and handled with care.

Syntheses. 2-Benzylsulfanylmethylpyrazine, L2. 2-(Chloromethyl)pyrazine (4.6 g, 35 mmol) was dissolved in ethanol (150 mL). Thiourea (2.7 g, 36 mmol) was added and the mixture was refluxed for 1 h. The solvent was removed, leaving the isothiuronium salt. The salt and excess KOH (4.6 g, 82 mmol) were dissolved in a 300-mL MeOH/H_2O (1:1 v/v) solution, were refluxed for 5 h, and were stirred overnight under argon. Argon-degassed CH_2Cl_2 (75 mL) was added via cannula to benzyl bromide (6.1 g, 36 mmol). This colorless solution was added to the black thiolate mixture, was refluxed for 5 h, and was stirred overnight under argon. The red/black solution was filtered and reduced in volume to a predominantly water solution. This was washed with CH_2Cl_2 (8 × 75 mL) and was dried ($MgSO_4$), and the solvent was removed again to give a crude black oil (6.3 g). Purification on a silica gel column (10% hydrated v/v) eluted with benzene gave **L2** as a yellow oil which crystallized on standing (1.8 g, 24%). NMR: ^{1}H ($CDCl_3$, 500 MHz, ppm) 8.52 (1H, br s, H(3)), 8.47 (1H, br s, H(6)), 8.41 (1H, br s, H(5)), 7.30 (2H, m, H(10)), 7.28 (2H, m, H(11), 7.22 (1H, m, H(12)), 3.71 (2H, s, H(7)), 3.69 (2H, s, H(8)); ^{13}C ($CDCl_3$, 500 MHz, ppm) 154.64 (C2), 144.81 (C3), 143.83 (C5), 142.75 (C6), 137.51 (C9), 129.01 (C10), 128.50 (C11), 127.15 (C12), 35.89 (C8), 34.45 (C7). Selected IR (neat)/cm^{-1}: 3060 (m), 3028 (m), 2922 (m), 1493 (s), 1472 (s), 1453 (s), 1399 (s), 1056 (s), 1017 (s), 700 (s). Found: C, 66.34; H, 5.70; N, 12.71; S, 14.64. Calcd for $C_{12}H_{12}N_2S$: C, 66.63; H, 5.59; N, 12.95; S, 14.82%.

Complexes. $\{$**[Co(L1)(MeCN)$_2$](ClO$_4$)$_2$**$\}_\infty$, **1.** $Co(ClO_4)_2 \cdot 6H_2O$ (94.7 mg, 0.26 mmol) dissolved in degassed MeCN (25 mL) was added via cannula to **L1** (54.5 mg, 0.25 mmol) dissolved in degassed MeCN (25 mL). The solution was left to stir overnight. The red-orange solution was reduced in volume to 5 mL and diethyl ether (50 mL) was added causing the formation of a tan precipitate. The powder was filtered and dried in vacuo. Yield 121.4 mg (89%). Orange X-ray quality crystals were grown from the slow diffusion of a $CHCl_3$ solution of **L1** (18.2 mg, 0.08 mmol) layered with ethyl acetate into a MeCN solution of $Co(ClO_4)_2 \cdot 6H_2O$ (31.8 mg, 0.09 mmol). Found: C, 29.13; H, 3.03; N, 14.64; S, 5.53. Calcd for $C_{10}H_{10}N_4SCoCl_2O_8 \cdot 2MeCN \cdot H_2O$: C, 29.18; H, 3.15; N, 14.58; S, 5.56%. MS (ESIMS$^+$) *m*/*z* (%): 376 (100) [Co(**L1**)ClO_4]$^+$ and 851 (30) [Co_2(**L1**)$_2$(ClO_4)$_3$]$^+$; selected IR (KBr): 2299 (m) (MeCN), 1412 (s) (**L1**), 1146 (s) 1089 (s) (ClO_4^-), 625 (s) cm^{-1}. UV−vis ($BaSO_4$) (relative absorption) 21 600 (100), 9320 (60), 6998 (39), 6064 (35), 5754 (36), 5181 (85) cm^{-1}; (MeCN) (ϵ/L mol^{-1} cm^{-1}) 22 400 (30), 9720 (4.4), 7107 (13), 5599 (4.0), 5249 (92) cm^{-1}.

$\{$**[Ni(L1)(NO$_3$)$_2$]**$\}_\infty$, **2.** $Ni(NO_3)_2 \cdot 6H_2O$ (69.5 mg, 0.24 mmol) dissolved in degassed MeCN (25 mL) was added via cannula to **L1** (50.5 mg, 0.23 mmol) dissolved in degassed MeCN (25 mL). The solution was left to stir overnight forming a green precipitate. The resultant suspension was reduced in volume to 10 mL, and the powder was filtered and dried in vacuo. Yield 77.0 mg (83%). Blue-green X-ray quality crystals were grown from the slow diffusion of a $CHCl_3$ solution of **L1** (21.8 mg, 0.09 mmol) layered with CH_2Cl_2 into a MeCN solution of $Ni(NO_3)_2 \cdot 6H_2O$ (31.7 mg, 0.11 mmol). Found: C, 26.47; H, 3.66; N, 18.42; S, 6.78. Calcd for $C_{10}H_{10}N_6SNiO_6 \cdot 3H_2O$: C, 26.40; H, 3.54; N, 18.47; S, 7.05%; selected IR (KBr): 1480−1270 (s, b) (NO_3^-), 1144 (s), 1081 (m),

(33) Amoore, J. J. M.; Black, C. A.; Hanton, L. R.; Spicer, M. D. *Cryst. Growth Des.* **2005**, *5*, 1255−1261.

Table 1

	1	2	3·H_2O	4·H_2O	5
formula	$C_{14}H_{16}CoN_6O_8SCl_2$	$C_{10}H_{10}NiN_6O_6S$	$C_{12}H_{17}Cd_2N_9O_{14}S$	$C_{12}H_{20}CoN_2O_{12}SCl_2$	$C_{12}H_{14}CdN_4O_7S$
formula weight	558.22	400.98	768.21	546.19	470.75
crystal system	monoclinic	monoclinic	monoclinic	triclinic	monoclinic
space group	$P2_1/c$	$P2_1/n$	$P2_1/c$	$P\bar{1}$	Cc
color	orange	pale green	colorless	light orange	colorless
a/Å	11.672(2)	8.8097(4)	7.42240(10)	7.018(5)	7.429(5)
b/Å	12.952(3)	14.2323(10)	26.3251(5)	7.443(5)	30.728(5)
c/Å	14.072(3)	11.2912(7)	13.7056(2)	19.420(5)	8.143(5)
α/deg	90	90	90	87.170(5)	90
β/deg	97.084(4)	92.835(4)	116.6530(10)	88.412(5)	116.802(5)
γ/deg	90	90	90	85.967(5)	90
V/Å^3	2111.1(14)	1413.98(15)	2393.44(7)	1010.4(10)	1659.2(15)
Z	4	4	4	2	4
T/K	113(2)	123(2)	123(2)	85(2)	85(2)
μ/mm^{-1}	1.221	1.566	1.951	1.282	1.486
reflections collected	13 434	8914	16 261	16 090	21 059
unique reflections (R_{int})	4278 (0.0456)	2491 (0.0647)	5362 (0.0554)	5396 (0.0572)	4422 (0.0205)
R_1 indices [$I > 2\sigma(I)$]	0.0438 (3142)	0.0397 (2019)	0.0565 (4573)	0.0430 (4355)	0.0168 (4266)
w$R2$ (all data)	0.1120	0.0942	0.1381	0.1209	0.0362
goodness-of-fit	1.045	1.087	1.214	1.122	1.051

1045 (s) (**L1**), 833 (m) cm^{-1}. UV−vis ($BaSO_4$) (relative absorption) 27 300 (1), 17 800 (0.34), 10 270 (0.37), 6028 (0.08), 5734 (0.07), 5179 (0.08) cm^{-1}.

{**[Cd_2(L1)(MeCN)(H_2O)(NO_3)$_4$]·H_2O**}$_\infty$, **3·H_2O.** $Cd(NO_3)_2$·$4H_2O$ (146.7 mg, 0.48 mmol) dissolved in degassed MeCN (25 mL) was added via cannula to **L1** (49.0 mg, 0.22 mmol) dissolved in degassed MeCN (25 mL). The solution was left to stir overnight. The resultant pale yellow solution was reduced in volume to 10 mL, and *n*-butanol (10 mL) was added as an aid to precipitation. The solution was then further reduced in volume to 10 mL causing the formation of a tan precipitate which was filtered and dried. Yield 21.6 mg (14%). White X-ray quality crystals were grown from the slow diffusion of a $CHCl_3$ solution of **L1** (21.6 mg, 0.10 mmol) layered with CH_2Cl_2 into a MeCN solution of $Cd(NO_3)_2$·$4H_2O$ (61.0 mg, 0.20 mmol). Found: C, 18.57; H, 2.16; N, 15.83; S, 4.20. Calcd for $C_{10}H_{10}N_8SCd_2O_{12}$·MeCN·$2H_2O$: C, 18.76; H, 2.23; N, 16.41; S, 4.17%; Selected IR (crystals) (KBr): 2299 (w) (MeCN), 1490−1270 (s, b) (NO_3^-), 1139 (m), 1075 (m), 1037 (s) (**L1**), 816 (m) cm^{-1}.

{**[Co(L2)(H_2O)$_3$](ClO_4)$_2$·H_2O**}$_\infty$, **4·H_2O.** $Co(ClO_4)_2$·$6H_2O$ (85 mg, 0.23 mmol) dissolved in degassed MeCN (25 mL) was added via cannula to **L2** (49 mg, 0.23 mmol) dissolved in MeCN (25 mL). The orange solution was stirred overnight and was concentrated to ∼10 mL. Diethyl ether (50 mL) was added resulting in the formation of a pink precipitate which was filtered and dried (0.10 g, 96%). Light-orange X-ray quality crystals were grown from the slow diffusion of a $CHCl_3$ solution of **L2** (20 mg, 0.092 mmol) layered with ethyl acetate into a MeCN solution of $Co(ClO_4)_2$·$6H_2O$ (38 mg, 0.10 mmol). Found (crystals): C, 26.07; H, 3.56; N, 4.89; S, 5.68. Calcd for $C_{12}H_{12}N_2SCoCl_2O_8$: C, 26.39; H, 3.69; N, 5.13; S, 5.87%. MS (ESIMS$^+$) *m*/*z* (%): 374 (100) [Co(**L2**)-ClO_4]$^+$ and 590 (35) [Co(**L2**)$_2ClO_4$]$^+$. Selected IR (KBr/crystals)/cm^{-1}: 1636 (m), 1491 (w) (**L2**), 1454 (w) (**L2**), 1418 (m), 1108 (s, br) (ClO_4^-), 698 (w) (**L2**), 626 (s) (ClO_4^-). UV−vis ($BaSO_4$) (relative absorption) 21 500 (100), 9440 (50), 7920 (54), 6645 (38), 5724 (21), 5530 (17) cm^{-1}; (MeCN) (ϵ/L mol^{-1} cm^{-1}) 21 050 (12), 9400 (3.4), 8430 (3.2) cm^{-1}.

{**[Cd(L2)(H_2O)(NO_3)$_2$]**}$_\infty$, **5.** $Cd(NO_3)_2$·$4H_2O$ (81 mg, 0.26 mmol) dissolved in degassed MeCN (25 mL) was added via cannula to **L2** (52 mg, 0.24 mmol) dissolved in MeCN (25 mL). The pale yellow solution was stirred overnight and was concentrated to ∼10 mL. Diethyl ether (50 mL) was added resulting in the formation of a brown precipitate which rapidly decomposed and could not be collected. White X-ray quality crystals were grown from the slow diffusion of a $CHCl_3$ solution of **L2** (21 mg, 0.095 mmol) layered with CH_2Cl_2 into a MeCN solution of $CdNO_3$·$4H_2O$ (42 mg, 0.14 mmol). Yield (crystals): 2.6 mg (2%). Selected IR (crystals) (KBr)/cm^{-1}: 3059 (w) (**L2**), 2916 (w) (**L2**), 1468 (m) (**L2**), 1384 (s) (NO_3^-), 1019 (w) (**L2**), 825 (w), 697 (w) (**L2**).

X−ray Crystallography. X-ray diffraction data were collected for **1** on a Bruker SMART CCD diffractometer, for **2** and **3·H_2O** on a Nonius Kappa-CCD diffractometer, and for **4·H_2O** and **5** on a Bruker APEX II CCD diffractometer, all with graphite monochromated Mo Kα (λ = 0.71073 Å) radiation. Intensities were corrected for Lorentz polarization effects[25] and a multiscan absorption correction[26] was applied to **1**, **4·H_2O**, and **5**. The structures were solved by direct methods (SHELXS[27] or SIR−97[28]) and were refined on F^2 using all data by full-matrix least-squares procedures (SHELXL 97[29]). All calculations were performed using the WinGX interface.[30] Detailed analyses of the extended structure were carried out using PLATON[31] and MERCURY[32] (Version 1.4.1). Crystal data and refinement details for the five structures are summarized in Table 1.

Results and Discussion

Synthesis and Structure of {[Co(L1)(MeCN)$_2$](ClO_4)$_2$}$_\infty$, 1. A bulk reaction with a 1:1 molar ratio of $Co(ClO_4)_2$·$6H_2O$ and **L1** yielded a tan solid. Microanalytical data were consistent with the solid having a 1:1 metal-to-ligand ratio. The solid was soluble in several polar organic solvents. Electrospray mass spectrometry under normal operating conditions in MeCN showed only two peaks with the correct isotopic patterns for [Co(**L1**)ClO_4]$^+$ at *m*/*z* 376 (100%) and [Co_2(**L1**)$_2$(ClO_4)$_3$]$^+$ at 851 (30%). These results pointed to a close association of ClO_4^- anion with the complex. The existence of the peak at *m*/*z* 851 indicated that **1** may exist as an oligomeric species in solution. There was no peak observed for the free ligand. The infrared spectrum recorded for crystalline material indicated the presence of MeCN and showed two strong peaks in the ClO_4^- stretching region at 1146 cm^{-1} and 1089 cm^{-1}. The electronic spectra of **1** measured in MeCN solution and the solid state displayed comparable features. This suggested similar primary coordination environments around the cobalt ion in the solid state

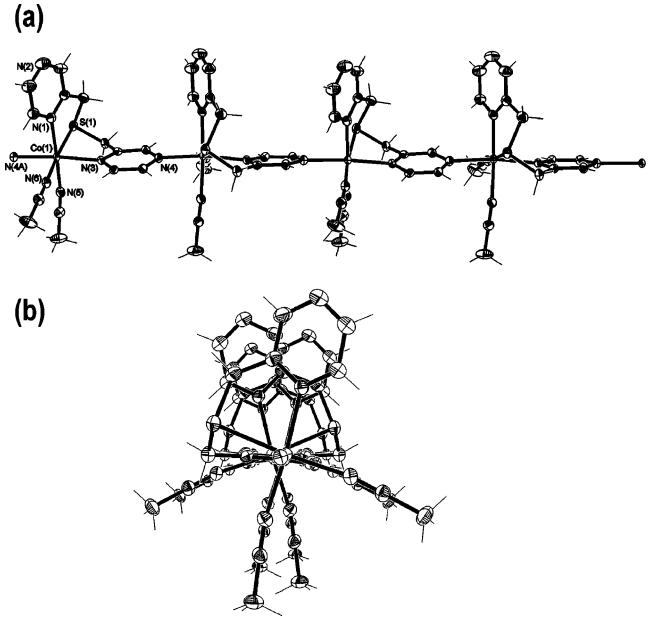

Figure 2. (a) View (*ac* plane) of a section of the polymeric 1-D chain formed in **1** showing crystallographic numbering. Thermal ellipsoids are drawn at the 50% probability level. The ClO_4^- anions are omitted for clarity. Selected bond lengths (Å) and angles (°): Co(1)−N(1) 2.119(3), Co(1)−N(3) 2.147(3), Co(1)−N(4A) 2.140(3), Co(1)−N(5) 2.092(3), Co(1)−N(6) 2.107(3), Co(1)−S(1) 2.4742(13), N(1)−Co(1)−N(3) 96.27(11), N(1)−Co(1)−N(4A) 91.71(11), N(1)−Co(1)−N(5) 174.31(12), N(1)−Co(1)−N(6) 95.50(12), N(1)−Co(1)−S(1) 80.51(9), N(3)−Co(1)−N(4A) 170.76(11), N(3)−Co(1)−N(5) 86.69(11), N(3)−Co(1)−N(6) 92.64(11), N(3)−Co(1)−S(1) 81.04(8), N(4A)−Co(1)−N(5) 84.97(11), N(4A)−Co(1)−N(6) 91.22(11), N(4A)−Co(1)−S(1) 95.75(8), N(5)−Co(1)−N(6) 89.20(12), N(5)−Co(1)−S(1) 95.20(9), N(6)−Co(1)−S(1) 172.06(9) (symmetry code: A x, $^1/_2 - y$, $z + ^1/_2$). (b) View along the *c*-axis showing the wagging along the chain in **1**.

and solution. The spectra were consistent with a high-spin Co(II) ion in a pseudo-octahedral environment with a large broad peak at (solid, solution) 9320, 9720 cm^{-1} assigned to the $^4T_{1g}(F) \rightarrow {}^4T_{2g}(F)$ transition and a shoulder at approximately 21600, 22400 cm^{-1} assigned to the $^4T_{1g}(F) \rightarrow {}^4T_{1g}(P)$ transition.

X-ray structural analysis of **1** revealed a slightly twisted 1-D chain running parallel to the *c*-axis. The asymmetric unit contained a Co(II) ion, a facially coordinated ligand **L1**, two cis bound MeCN ligands, and two ClO_4^- counterions. The 1-D chain was formed by linking two symmetry related asymmetric units through one of the pyrazine groups of **L1** (Figure 2a) through a *c*-glide plane. The other pyrazine ring was not involved in a bridging interaction with a Co(II) center. Thus, every other unit along the chain was reflected through this plane such that alternating asymmetric units were related to each other as enantiomers, with S donors arranged on opposite sides of the chain. One of the MeCN ligands also alternated in this way. This arrangement gave rise to a wagging of the other MeCN ligand, the remaining pyrazine group, and both of the ClO_4^- anions along the chain (Figure 2b). The Co(II) cation adopted a pseudo-octahedral arrangement with bridging pyrazine rings trans to one another. The facially bound **L1** assumed a twisted endo−syn conformation[33] with the S donor and nonbridged pyrazine ring each trans to a different MeCN ligand. A search of the Cambridge Crystallographic Database (CSD version 5.27)[34] revealed that

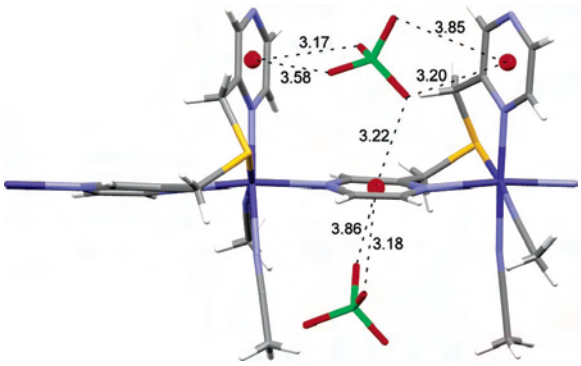

Figure 3. View (*ac* plane) of the U-shaped cavity and anion−π interactions formed in **1**.

all bond lengths about the central Co(II) cation were within the normal ranges [Co−SC_2 2.132−2.729 Å; Co−N(pyrazine) 1.844−2.259 Å; Co−$NCCH_3$ 1.883−2.269 Å]. One of the remarkable features of this structure was the encapsulation of one of the ClO_4^- anions in a U-shaped cavity formed by three pyrazine rings between two Co(II) centers of the polymer chain (Figure 3). The ClO_4^- anion was held in place by a total of five anion−π interactions (Table 2) where one anion O atom [O(12)] was found to interact with two pyrazine rings from the same ligand. All four O atoms of this ClO_4^- anion were involved in anion−π interactions. In two cases, two O atoms interacted with the same ring. Also notable were the two anion−π interactions formed between the bridging pyrazine ring and the other ClO_4^- counterion (Figure 3). The counterion had three supplementary Cl−O···H−C (sp^3) interactions of about 2.7 Å [corresponding O···C separations were about 3.3 Å]. Thus, the bridging pyrazine ring was sandwiched between the two ClO_4^- anions. Additional support for this close association was provided by the retention of ClO_4^- anions in species observed in the electrospray mass spectrum. The overall three-dimensional structure appeared in the main to be held together by a series of interchain Cl−O···H interactions in the range 2.45−2.70 Å [corresponding O···C separations were in the range 3.19−3.44 Å]. The noncoordinated N donor [N(2)] of the nonbridging pyrazine group was not involved in any significant interactions.

Synthesis and Structure of $\{[Ni(L1)(NO_3)_2]\}_\infty$, 2. A reaction using a 1:1 molar ratio of $Ni(NO_3)_2 \cdot 6H_2O$ and **L1** yielded a green powder which had a microanalysis consistent with the solid having a 1:1 metal-to-ligand ratio. It was insoluble in all common organic solvents. The infrared spectrum recorded for bulk material indicated the presence of ligand and showed a strong broad peak in the NO_3^- stretching region. The solid-state electronic spectrum of **2** was consistent with a Ni(II) ion in a pseudo-octahedral environment. It showed three main d−d bands at 10 270 cm^{-1} assigned to the $^3A_{2g}(F) \rightarrow {}^3T_{2g}(F)$ transition and shoulders at approximately 17 800 and 27 300 cm^{-1} assigned to the $^3A_{2g}(F) \rightarrow {}^3T_{1g}(F)$ and $^3A_{2g}(F) \rightarrow {}^3T_{1g}(P)$ transitions,

(34) Allen, F. H.; Davies, J. E.; Galloy, J. J.; Johnson, O.; Kennard, O.; Macrae, C. F.; Mitchell, E. M.; Mitchell, G. F.; Smith, J. M.; Watson, D. G. *J. Chem. Inf. Comput. Sci.* **1991**, *31*, 187−204.

Table 2. Analysis of Anion−π Interactions (Distances, Å; Angles, °) for Compounds **1**−**5**

compound	interaction	X = ring centroid	X = ring plane	angle between O···X axis and ring plane (X = ring centroid)	X = closest ring atom
1[c]	Cl(1)−O(11)···X	3.166(5)	3.13	81.3	3.231(6) (C2A)
	Cl(1)−O(12)···X	3.219(4)	2.90[a]	64.3	2.908(5) (C10)
		3.203(5)	3.02	70.5	3.074(6) (C4)
	Cl(1)−O(13)···X	3.582(5)	3.06[a]	58.6	3.102(6) (C4A)
	Cl(1)−O(14)···X	3.848(4)	3.49[a]	65.2	3.564(6) (C3)
	Cl(2)−O(23)···X	3.855(4)	2.76[b]	45.6	3.177(5) (C8)
	Cl(2)−O(24)···X	3.182(4)	3.15	81.9	3.269(5) (C8)
2[d]	N(5)−O(51)···X	3.397(3)	2.98[a]	61.5	3.081(4) (C2A)
	N(5)−O(53)···X	3.674(3)	2.97[b]	53.8	3.184(5) (C1A)
	N(6)−O(62)···X	3.825(3)	3.35[a]	61.1	3.488(4) (C4A)
	N(6)−O(63)···X	3.690(3)	2.70[b]	47.0	2.980(4) (C10B)
3·H$_2$O[e]	N(21)−O(22)···X	3.519(7)	2.73[b]	51.0	2.884(8) (N3)
		3.637(6)	2.73[b]	48.6	3.052(10) (C4C)
	N(21)−O(23)···X	3.133(7)	3.07	78.3	3.172(10) (C3C)
	N(41)−O(42)···X	3.265(7)	3.26	88.5	3.503(10) (C4A)
	N(41)−O(43)···X	3.096(6)	3.00	75.9	3.075(10) (C10A)
		3.825(7)	2.85[b]	48.3	3.195(10) (C2B)
		3.859(7)	3.14[b]	54.5	3.350(10) (C4A)
4·H$_2$O	Cl(1)−O(11)···X	2.990(3)	2.93	78.0	3.028(4) (N2)
	Cl(1)−O(13)···X	3.676(4)	3.22[a]	61.2	3.272(5) (C4)
	Cl(2)−O(22)···X	3.232(4)	3.12	75.0	3.189(5) (C1)
	Cl(2)−O(23)···X	3.424(4)	3.07[a]	63.8	3.139(5) (C3)
	Cl(2)−O(24)···X	3.766(4)	3.12[a]	56.0	3.223(5) (C2)
5[f]	N(3)−O(32)···X	3.048(3)	2.84	68.6	2.845(4) (C4A)
	N(4)−O(41)···X	3.107(3)	3.05	78.9	3.135(3) (C1B)

[a] Contact with plane was <0.7 Å outside the pyrazine ring. [b] Contact with plane was >0.7 Å outside the pyrazine ring. [c] Symmetry code for **1**: A x, $^1/_2 - y$, $z - ^1/_2$. [d] Symmetry code for **2**: A $^1/_2 - x$, $^1/_2 + y$, $^1/_2 - z$; B $1 + x$, y, z. [e] Symmetry code for **3·H$_2$O**: A $-x$, $1 - y$, $1 - z$; B $-1 - x$, $1 - y$, $1 - z$; C x, $^1/_2 - y$, $z - ^1/_2$. [f] Symmetry code for **5**: A x, y, $z - 1$; B $1 + x$, y, $1 + z$.

respectively.[35] The latter transitions were somewhat obscured by a large charge-transfer band starting around 11 000 cm^{-1}.

X-ray structural analysis showed that **2** formed an undulating 1-D chain running parallel to the [1 0 1] diagonal axis. The asymmetric unit contained a Ni(II) ion, a facially coordinated ligand **L1**, and two cis bound NO_3^- anions. The 1-D chain was formed by linking two symmetry related asymmetric units through one of the pyrazine groups of **L1** (Figure 4a) through an *n*-glide plane. Thus, every alternate unit along the chain was reflected through this glide plane such that the S donors were on the same side of the chain and the nonbridging pyrazine rings were approximately 150° to each other (Figure 4b). A pseudo-octahedral geometry was adopted by the Ni(II) cation in which the bridging pyrazine rings were arranged trans to one another. The facially bound **L1** had a twisted endo−syn conformation[33] with the S donor and nonbridged pyrazine ring each trans to different bound NO_3^- anions. A search of the CSD[34] revealed that all bond lengths about the central Ni(II) cation were within the normal ranges [Ni−SC$_2$ 2.087−2.943 Å; Ni−N(pyrazine) 1.855−2.266 Å; Ni−ONO$_2$ 1.925−2.280 Å]. The packing of the 1-D chains showed unusual pyrazine π interactions. Adjacent chains were interdigitated through one face-to-face [centroid-to-centroid distance 3.49 Å][16,36] and two complementary T-shaped π interactions generating a two-dimensional sheet in the (−1 0 1) plane (Figure 5). Notably, the T-shaped interaction involved the N donor of the nonbridged pyrazine interacting with the electron-deficient bridging pyrazine ring [N(pyrazine)···centroid(pyrazine) distance 3.05 Å, angle

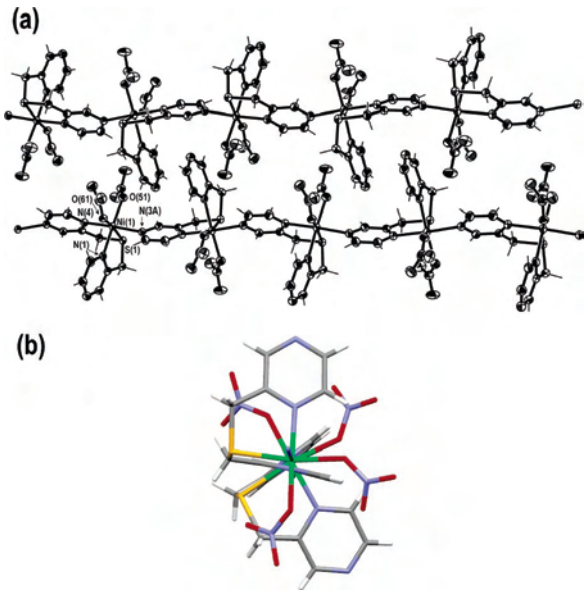

Figure 4. (a) View (crystallographic numbering) of two polymeric chains in **2** running parallel to the [1 0 1] axis. Thermal ellipsoids are drawn at the 50% probability level. Selected bond lengths (Å) and angles (°): Ni(1)−N(1) 2.100(3), Ni(1)−N(3A) 2.125(3), Ni(1)−N(4) 2.113(3), Ni(1)−O(51) 2.043(2), Ni(1)−O(61) 2.070(2), Ni(1)−S(1) 2.3886(10); N(1)−Ni(1)−N(3A) 90.83(11), N(1)−Ni(1)−N(4) 87.58(11), N(1)−Ni(1)−O(51) 176.48(9), N(1)−Ni(1)−N(61) 86.95(10), N(1)−Ni(1)−S(1) 84.36(8), N(3A)−Ni(1)−N(4) 174.95(11), N(3A)−Ni(1)−O(51) 86.19(10), N(3A)−Ni(1)−O(61) 86.85(10), N(3A)−Ni(1)−S(1) 90.70(8), N(4)−Ni(1)−O(51) 95.55(10), N(4)−Ni(1)−O(61) 97.85(10), N(4)−Ni(1)−S(1) 84.37(8), O(51)−Ni(1)−O(61) 91.01(10), O(51)−Ni(1)−S(1) 97.55(7), O(61)−Ni(1)−S(1) 170.93(7) (symmetry code: A $x + ^1/_2$, $^1/_2 - y$, $z + ^1/_2$). (b) View showing the 150° rotation of pyrazine rings along the chain in **2**.

(35) (a) Cooper, S. R.; Rawle, S. C.; Hartman, J. R.; Hintsa, E. J.; Admans, G. A. *Inorg. Chem.* **1988**, *27*, 1209−1214. (b) Adhikary, B.; Liu, S.; Lucas, C. R. *Inorg. Chem.* **1993**, *32*, 5957−5962.

(36) (a) Hunter, C. A. *Chem. Soc. Rev.* **1994**, *23*, 101−109. (b) Hunter, C. A.; Sanders, J. K. M. *J. Am. Chem. Soc.* **1990**, *112*, 5525−5534.

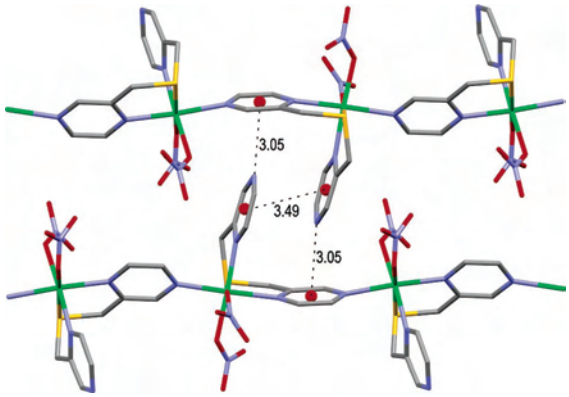

Figure 5. View of the chain formed in **2** showing complementary face-to-face and T-shaped π interactions between chains. Hydrogen atoms are omitted for clarity.

between pyrazine ring planes 71.2°] in contrast to the commonly observed C(arene)−H···arene interaction.[37] This N···π(pyrazine) distance is shorter than the van der Waals distance (3.40 Å) on the basis of Pauling's value for the half thickness of a phenyl ring (1.85 Å)[38] and the van der Waals radius of N (1.55 Å).[39] To our knowledge, this type of T-shaped heteroaromatic interaction has never been commented upon before. A search of the CSD was carried out using the following constraints. The distance between a N donor and a centroid of two six-membered heteroaromatic rings in the range 2.00−3.40 Å and the angle between the planes of the two rings in the range 60−90° were analyzed. This analysis revealed 33 examples with an average N··· centroid distance of 3.17 Å and an average angle between the planes of 80.0°.[40] The shortest distance found was 2.98 Å at an angle of 82.2°,[41] with the longest distance being 3.37 Å at an angle of 81.4°.[42] The interdigitated chains also displayed three anion−π interactions (Table 2; Figure 6). Three of the O atoms of the two bound NO_3^- anions on one chain interacted with a pyrazine ring on the other chain. In addition, two chains in adjacent sheets were bridged by one of these NO_3^- anions through an anion−π interaction (Table 2; Figure 5). These π interactions were supplemented by a series of N−O···H interactions in the range 2.21−2.58 Å (corresponding O···C separations were in the range 2.92−3.50 Å) forming the overall three-dimensional structure.

Synthesis and Structure of {[Cd_2(L1)(MeCN)(H_2O)(NO_3)$_4$]·H_2O}$_\infty$, 3·H_2O. A 1:1 molar reaction between Cd(NO_3)$_2$·4H_2O and **L1** gave a light-brown product in low yield when precipitated from diethyl ether. The product decomposed slowly with time. When a 2:1 metal-to-ligand molar ratio was employed, a similar result was obtained. Microanalytical data for both materials were ambiguous with analyses giving values between those expected for a 1:1 and 2:1 metal-to-ligand molar ratio for the solid. In an attempt to prepare microanalytically pure material from a 2:1 metal-to-ligand molar reaction, *n*-butanol was used rather than diethyl ether to isolate a stable precipitate in low yield. The isolated product had a microanalysis consistent with a 1:1 molar ratio. Interestingly, X-ray quality crystals with a 2:1 metal-to-ligand ratio were obtained exclusively despite numerous crystallization attempts.

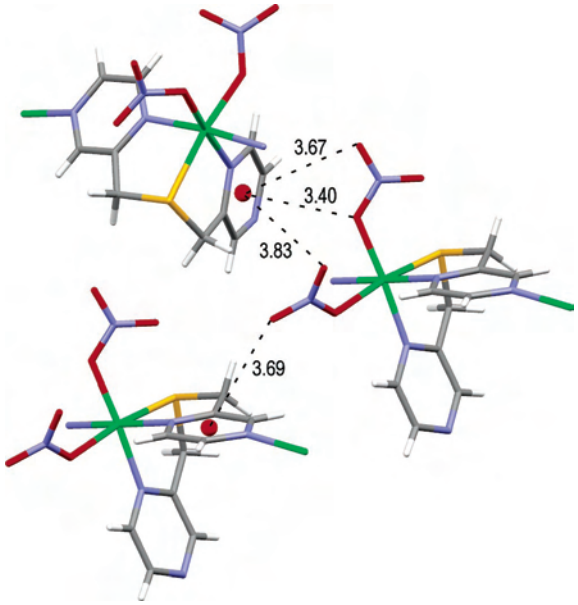

Figure 6. View of the anion−π interactions between three chains in **2**.

X-ray structural analysis of these crystals revealed a 1-D chain decorated with a Cd(II) moiety of bound anions and solvents running along the *a*-axis. The asymmetric unit consisted of two Cd(II) ions, a ligand **L1**, four bound NO_3^- anions, a MeCN and water ligand, and a free water molecule. The 1-D chain was formed by linking two symmetry related asymmetric units through one of the pyrazine groups of **L1** through a cell translation (Figure 7). The Cd(II) ion generating the chain was seven-coordinate and was linked by trans bridging pyrazine rings. This Cd(II) ion had a facially bound ligand **L1** with a twisted endo−syn conformation[33] and two cis coordinated NO_3^- anions. The NO_3^- anion trans to the S donor was bidentate while the other NO_3^- anion was monodentate. The nature of the binding of these anions was unambiguous as defined by their Cd−O distances (Figure 7). Although one of the NO_3^- anions was bidentate, it had a small bite angle and effectively occupied only one coordination site, allowing for a pseudo-octahedral description of the geometry about the Cd(II) cation. The pyrazine ring not involved in propagating the 1-D polymer was bound to a seven-coordinate Cd(II) moiety which decorated one side of the chain. Trans to one another were MeCN and water ligands and two bidentate NO_3^- anions. The small bite angles

(37) Nishio, M. *CrystEngComm* **2004**, *6*, 130−158.
(38) Malone, J. F.; Murray, C. M.; Charlton, M. H.; Docherty, R.; Lavery, A. J. *J. Chem. Soc., Faraday Trans.* **1997**, *93*, 3429−3436.
(39) Bondi, A. *J. Phys. Chem.* **1964**, *68*, 441−51.
(40) For examples see: Berthet, J.−C.; Miquel, Y.; Iveson, P. B.; Nierlich, M.; Thuery, P.; Madic, C.; Ephritikhine, M. *J. Chem. Soc., Dalton Trans.* **2002**, 3265−3272. McMurran, J.; Kouvetakis, J.; Nesting, D. C.; Hubbard, J. L. *Chem. Mater.* **1998**, *10*, 590−593. Childs, B. J.; Cadogan, J. M.; Craig, D. C.; Scudder, M. L.; Goodwin, H. A. *Aust. J. Chem.* **1997**, *50*, 129−138. Piccinni-Leopardi, C.; Van Meerssche, M.; Declerq, J. P.; Germain, G. *Bull. Soc. Chim. Belg.* **1987**, *96*, 79−80.
(41) Blake, A. J.; Brooks, N. R.; Champness, N. R.; Cooke, P. A.; Deveson, A. M.; Fenske, D.; Hubberstey, P.; Li, W.−S.; Schroder, M. *J. Chem. Soc., Dalton Trans.* **1999**, 2103−2110.
(42) Morgado, J.; Santos, I. C.; Veiros, L. F.; Rodrigues, C.; Henriques, R. T.; Duarte, M. T.; Alcacer, L.; Almeida, M. *J. Mater. Chem.* **2001**, *11*, 2108−2117.

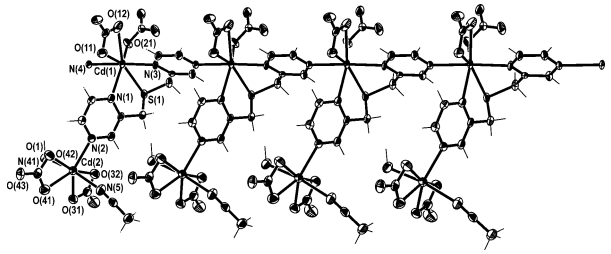

Figure 7. View (crystallographic numbering) of the polymeric chain of **3·H₂O**, illustrating the decorated Cd(II) moiety. The noncoordinated water molecule is omitted for clarity. Thermal ellipsoids are drawn at the 50% probability level. Selected bond lengths (Å) and angles (°): Cd(1)−N(1) 2.438(6), Cd(1)−N(3) 2.311(5), Cd(1)−N(4A) 2.363(5), Cd(1)−O(11) 2.463(6), Cd(1)−O(12) 2.539(7), Cd(1)−O(21) 2.317(5), Cd(1)−S(1) 2.7371(18), Cd(2)−N(2) 2.305(6), Cd(2)−N(5) 2.343(6), Cd(2)−O(1) 2.299(5), Cd(2)−O(31) 2.335(5), Cd(2)−O(32) 2.435(6), Cd(2)−O(41) 2.380(6), Cd(2)−O(42) 2.456(6); N(1)−Cd(1)−N(3) 93.52(19), N(1)−Cd(1)−N(4A) 83.45(19), N(1)−Cd(1)−O(11) 77.65(19), N(1)−Cd(1)−O(12) 127.8(2), N(1)−Cd(1)−O(21) 147.9(2), N(1)−Cd(1)−S(1) 72.69(14), N(3)−Cd(1)−N(4A) 177.0(2), N(3)−Cd(1)−O(11) 93.69(19), N(3)−Cd(1)−O(12) 85.61(19), N(3)−Cd(1)−O(21) 104.69(19), N(3)−Cd(1)−S(1) 76.38(15), N(4A)−Cd(1)−O(11) 85.55(19), N(4A)−Cd(1)−O(12) 96.14(19), N(4A)−Cd(1)−O(21) 78.08(19), N(4A)−Cd(1)−S(1) 102.75(14), O(11)−Cd(1)−O(12) 50.50(19), O(11)−Cd(1)−O(21) 126.1(2), O(11)−Cd(1)−S(1) 147.90(13), O(12)−Cd(1)−O(21) 80.5(2), O(12)−Cd(1)−S(1) 153.95(14), O(21)−Cd(1)−S(1) 85.98(15), N(2)−Cd(2)−N(5) 91.3(2), N(2)−Cd(2)−O(1) 97.2(2), N(2)−Cd(2)−O(31) 137.6(2), N(2)−Cd(2)−O(32) 84.0(2), N(2)−Cd(2)−O(41) 135.0(2), N(2)−Cd(2)−O(42) 82.7(2), N(5)−Cd(2)−O(1) 170.4(2), N(5)−Cd(2)−O(31) 84.6(2), N(5)−Cd(2)−O(32) 86.4(2), N(5)−Cd(2)−O(41) 91.8(2), N(5)−Cd(2)−O(42) 105.2(2), O(1)−Cd(2)−O(31) 86.10(19), O(1)−Cd(2)−O(32) 90.01(19), O(1)−Cd(2)−O(41) 85.3(2), O(1)−Cd(2)−O(42) 80.39(19), O(31)−Cd(2)−O(32) 53.69(18), O(31)−Cd(2)−O(41) 87.37(19), O(31)−Cd(2)−O(42) 138.99(18), O(32)−Cd(2)−O(41) 141.03(19), O(32)−Cd(2)−O(42) 162.48(19), O(41)−Cd(2)−O(42) 53.23(19) (symmetry code: A $x-1, y, z$).

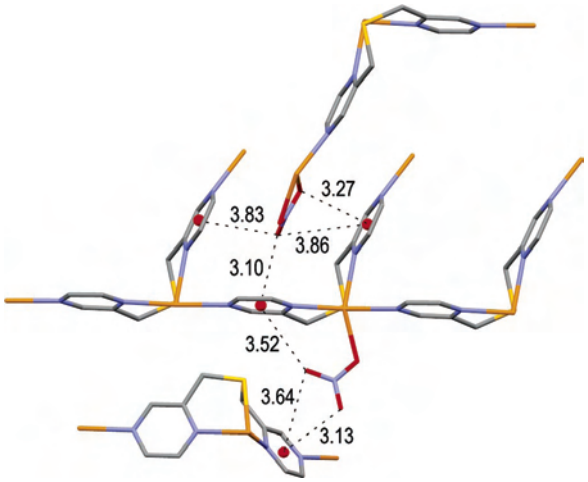

Figure 8. View of the U-shaped cavity and anion−π interactions between three chains in **3·H₂O**. Hydrogen atoms and selected anions are omitted for clarity.

of the NO_3^- anions allowed a pseudo-square−pyramidal description of the Cd(II) geometry with the pyrazine N donor at the apex of the pyramid. A search of the CSD[34] revealed that bond lengths about the Cd(II) cations were within the normal ranges (Cd−SC_2 2.574−2.982 Å; Cd−N(pyrazine) 2.326−2.526 Å; Cd−ONO_2 2.023−2.917 Å; Cd−OH_2 2.104−2.619 Å). The individual decorated chains were formed into a three-dimensional structure principally through seven anion−π interactions (Table 2; Figure 8). The monodentate anion was involved in two intermolecular interactions with a pyrazine ring of the decoration in an adjacent chain as well as an intramolecular interaction. One of the bidentate NO_3^- anions [N(41)] of the decoration was encapsulated in a U-shaped cavity formed by three pyrazine rings between two Cd(II) centers of an adjacent polymer chain. The NO_3^- anion was involved in a total of four anion−π interactions where one anion O atom [O(43)] was found to interact with all three pyrazine rings of the U-shaped cavity. The fourth NO_3^- interaction involved an O atom [O(42)] almost directly over the centroid of one of the pyrazine rings in the cavity such that this NO_3^- anion was almost parallel to the plane of the ring. In addition to these anion−π interactions, a series of H-bonding interactions, principally involving the bound H_2O ligand and NO_3^- anions, completed the overall three-dimensional structure (O···H interactions in the range 1.85−2.59 Å).

Synthesis and Structure of {[Co(L2)(H₂O)₃](ClO₄)₂·H₂O}∞, 4·H₂O. A 1:1 molar reaction between $Co(ClO_4)_2 \cdot 6H_2O$ and **L2** gave a pink product in high yield. Microanalytical data were consistent with the solid having a 1:1 metal-to-ligand ratio and four H_2O molecules. It was soluble in several polar organic solvents. Only two peaks were observed in the electrospray mass spectrum collected under normal operating conditions in MeCN. These peaks had the correct isotopic patterns for $[Co(\mathbf{L1})ClO_4]^+$ at *m*/*z* 374 (100%) and $[Co(\mathbf{L1})_2ClO_4]^+$ at 590 (35%). The infrared spectrum showed peaks which were assigned to the ligand as well as a strong broad peak assigned to a ClO_4^- stretch. For **4·H₂O** the electronic spectra, measured in MeCN solution and the solid state, were comparable. They showed high-spin Co(II) ions in pseudo-octahedral environments with a large broad peak, which was split in the solid state, at (solid; solution) 9440, 7920; 9400 cm^{-1} assigned to the $^4T_{1g}(F) \rightarrow {}^4T_{2g}(F)$ transition. A peak at 21 500; 21 050 cm^{-1} was assigned to the $^4T_{1g}(F) \rightarrow {}^4T_{1g}(P)$ transition. Therefore, in MeCN solution, a pseudo-octahedral geometry appeared to be maintained for the Co(II) ion.

The X-ray structure of **4·H₂O** showed a 1-D polymer chain directed along the *a*-axis. The asymmetric unit consisted of one Co(II) ion, a ligand **L2**, three bound water ligands, a free water molecule, and two noncoordinating ClO_4^- counter anions. The 1-D chain was formed by linking two symmetry related asymmetric units through a cell translation such that the Co(II) ion was pseudo-octahedral and was linked by trans bridging pyrazine rings of **L2** (Figure 9). The bidentate-bound **L2** had an endo−anti conformation[33] with the benzene ring oriented out from the chain. The three H_2O ligands were coordinated in a meridional fashion. The trans bridging pyrazine rings were sandwiched between two independent ClO_4^- anions which were directly above and below the ring centroid [Cl(1)−centroid−Cl(2) 175.2°]. In total, there were five anion−π interactions (Table 2; Figure 10) one of which had a short O(11)···centroid distance of 2.99 Å. A two-dimensional sheet was loosely formed in the *ab* plane by two distinct benzene $\pi-\pi$ interactions [centroid-to-centroid distances 3.81 and 3.98 Å][36] which arose from the interdigitation of adjacent chains (Figure 11). The water ligand trans to the S donor was arranged on the surface of the sheet and

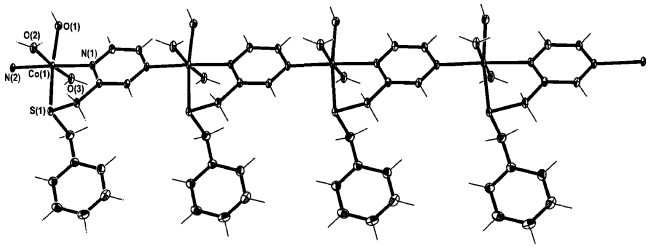

Figure 9. View (*ac* plane) of **4·H$_2$O** showing the coordination environment (crystallographic numbering) of the Co(II) ion and the 1-D chain. The noncoordinated H_2O molecule and the ClO_4^- anions are omitted for clarity. Thermal ellipsoids are drawn at the 50% probability level. Selected bond lengths (Å) and angles (°): Co(1)−N(1) 2.116(3), Co(1)−N(2A) 2.129(3), Co(1)−O(1) 2.120(3), Co(1)−O(2) 2.085(3), Co(1)−O(3) 2.060(3), Co(1)−S(1) 2.4893(11); N(1)−Co(1)−N(2A) 177.72(11), N(1)−Co(1)−O(1) 90.25(10), N(1)−Co(1)−O(2) 91.07(10), N(1)−Co(1)−O(3) 88.25(10), N(1)−Co(1)−S(1) 80.88(8), N(2A)−Co(1)−O(1) 92.02(10), N(2A)−Co(1)−O(2) 88.86(10), N(2A)−Co(1)−O(3) 92.06(10), N(2A)−Co(1)−S(1) 96.84(8), O(1)−Co(1)−O(2) 86.92(10), O(1)−Co(1)−O(3) 87.13(10), O(1)−Co(1)−S(1) 169.50(7), O(2)−Co(1)−O(3) 174.01(10), O(2)−Co(1)−S(1) 87.63(8), O(3)−Co(1)−S(1) 98.13(8) (symmetry code: A $x-1$, y, z).

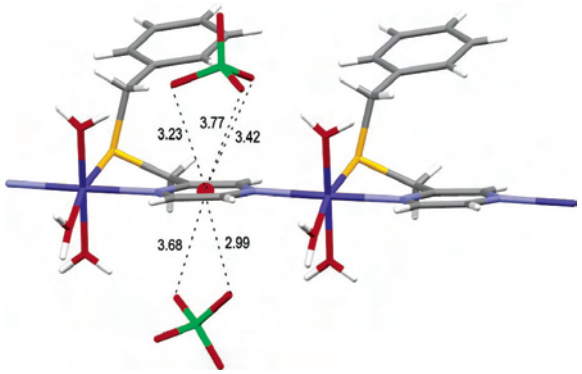

Figure 10. View of the anion−π−anion sandwich interaction in **4·H$_2$O**.

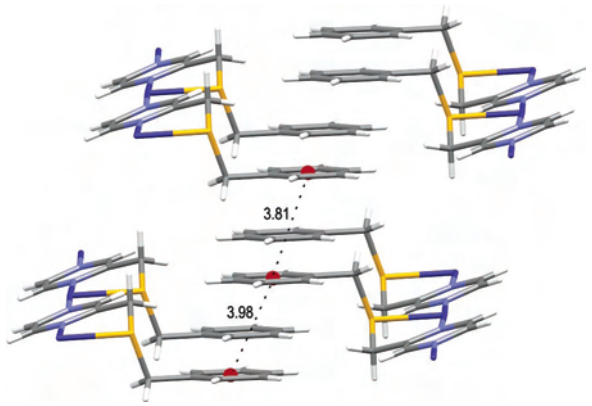

Figure 11. View of **4·H$_2$O** showing the interdigitation of benzene rings between adjacent chains. The ClO_4^- anions and H_2O ligands are omitted for clarity.

was involved in a series of H-bonding interactions involving the anions and the free water which stitched together the sheets producing the overall three-dimensional structure.

Synthesis and Structure of {[Cd(L2)(H$_2$O)(NO$_3$)$_2$]}$_\infty$, 5. A 1:1 molar reaction between $Cd(NO_3)_2{\cdot}4H_2O$ and **L2** resulted in the formation of a brown precipitate. The precipitate was impossible to recover as it always rapidly decomposed to a sticky oil. However, in attempting to crystallize the bulk material, white X-ray quality crystals

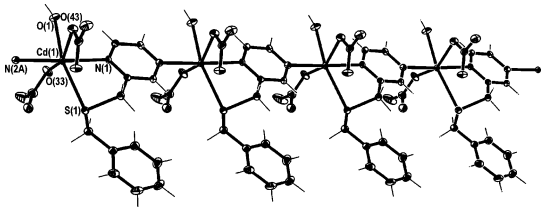

Figure 12. View (*ab* plane) of **5** showing the coordination environment (crystallographic numbering) of the Cd(II) ion and the 1-D chain. Thermal ellipsoids are drawn at the 50% probability level. Selected bond lengths (Å) and angles (°): Cd(1)−N(1) 2.360(3), Cd(1)−N(2A) 2.304(3), Cd(1)−O(1) 2.3021(12), Cd(1)···O(31) 3.069(3), Cd(1)−O(33) 2.309(2), Cd(1)···O(42) 3.019(2), Cd(1)−O(43) 2.338(2), Cd(1)−S(1) 2.6750(6); N(1)−Cd(1)−N(2A) 177.59(8), N(1)−Cd(1)−O(1) 88.88(7), N(1)−Cd(1)−O(33) 88.02(9), N(1)−Cd(1)−O(43) 93.21(9), N(1)−Cd(1)−S(1) 75.69(4), N(2A)−Cd(1)−O(1) 88.96(7), N(2A)−Cd(1)−O(33) 92.55(9), N(2A)−Cd(1)−O(43) 85.23(9), N(2A)−Cd(1)−S(1) 106.49(4), O(1)−Cd(1)−O(33) 77.79(8), O(1)−Cd(1)−O(43) 75.86(7), O(1)−Cd(1)−S(1) 164.53(6), O(33)−Cd(1)−O(43) 153.59(5), O(33)−Cd(1)−S(1) 100.30(5), O(43)−Cd(1)−S(1) 105.57(5) (symmetry code: A $x+1$, y, z).

were obtained in very low yield. The crystals were air stable and did not decompose, suggesting that they were not the same as the bulk material. The very low yield also indicated they may be a byproduct. Infrared spectral analysis of the crystals showed peaks at 3059, 2916, and 1468 cm^{-1} consistent with the ligand, and a strong peak at 1384 cm^{-1} assigned to NO_3^-. A consistently low crystal yield and a lack of bulk material precluded any microanalytical results.

Structural analysis of **5** showed a 1-D polymer chain running along the *a*-axis. The asymmetric unit consisted of a Cd(II) ion, two bound monodentate NO_3^- anions, a **L2** ligand, and a H_2O ligand. The pseudo-octahedral Cd(II) ions were chelated by the N and S donors of **L2**, with the H_2O ligand trans to the S donor. The NO_3^- anions were trans to each other and Cd···O contact distances clearly indicated that they were both monodentate (Figure 12). The remaining coordination site was occupied by a monodentate N donor from a pyrazine ring which bridged two Cd(II) centers in a trans fashion. In this way, the polymer chain was generated through a lattice translation of the asymmetric unit. The ligand **L2** adopted an endo−anti configuration in which the benzene rings were oriented away from the polymer chain in a similar manner to **4·H$_2$O**. This arrangement caused the S donors and benzene rings to be on only one side of the polymer chain. The trans NO_3^- anions were each involved in two interactions which generated a two-dimensional sheet in the *ac* plane (Figure 13). The sheet was made up of two layers with each layer the width of two chains and had benzene rings oriented on both surfaces. Each layer was generated by the first type of interaction which involved complementary anion−π interactions with the pyrazine rings of adjacent chains such that the NO_3^- anions were interdigitated and acted as supramolecular synthons. The two layers were stitched together by the second type of interaction which involved complementary H-bonding interactions between H_2O ligands of one layer and NO_3^- ligands of the other (N−O···H−O distances were 1.97 and 2.04 Å with corresponding O···O distances of 2.774(3) and 2.822(3) Å). The benzene rings oriented on both surfaces of the sheet were interdigitated with benzene rings on adjacent sheets completing the overall three-dimensional structure (Figure

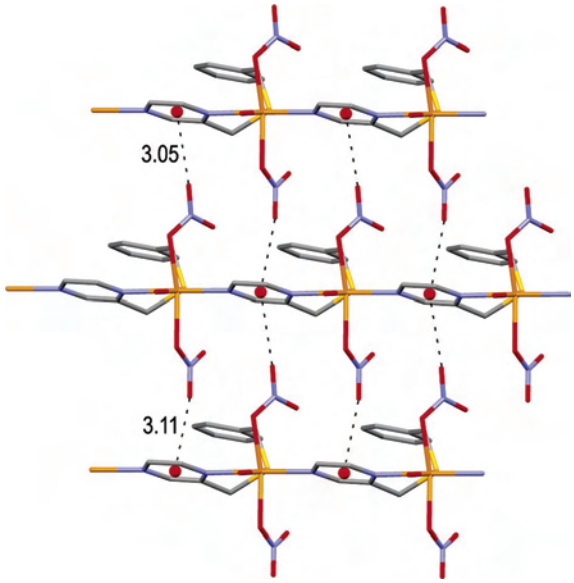

Figure 13. View of the anion−π interactions acting as supramolecular synthons between chains in **5**. Hydrogen atoms are omitted for clarity.

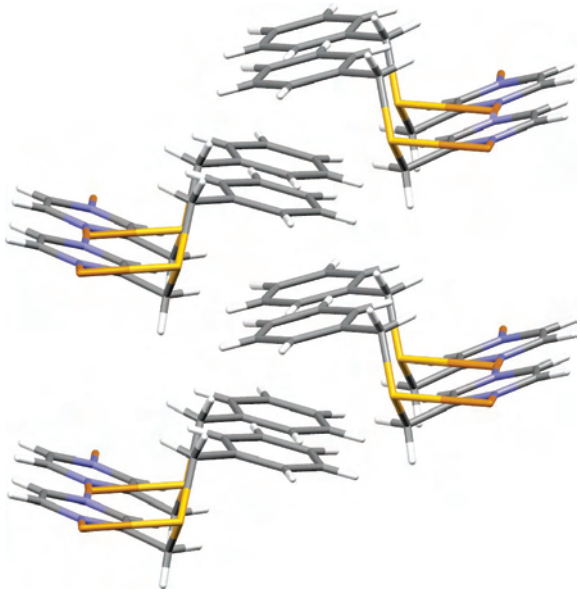

Figure 14. View of **5** showing the interdigitation of benzene rings between adjacent chains. The NO_3^- anions and H_2O ligands are omitted for clarity.

14). Despite this interdigitation, the benzene rings did not appear to participate in any obvious intermolecular interactions. The centroid-to-centroid distance was 4.17 Å[36] with an angle between ring planes of 24.6°.

Comparison. All five complexes were found to give 1-D linear coordination polymers. The polymers **1** and **4·H₂O** contained noncoordinated ClO_4^- anions while **2**, **3·H₂O**, and **5** contained bound NO_3^- anions. Thus, the anion−π interactions found for **1**−**5** occurred in both cationic and neutral 1-D coordination polymer chains. It was found that the strength of interaction appeared to be independent of the charge of the chain. This is somewhat surprising as it might be expected that a coordinated anion would be less electron rich and would therefore have weaker interactions with π-acidic centers. The range of O-to-centroid distance was found to vary from 2.99 to 3.86 Å. Longer anion−π distances might be expected as ClO_4^- and NO_3^- are delocalized anions resulting in the oxygen van der Waals radii being less than that found for simple anions like the halogens. However, typically the longer values were associated with other shorter O-to-centroid distances reflecting the asymmetry and complexity of the placement of the anions in the π pockets. In the coordination polymers, each ligand displayed a remarkable consistency of conformation for such flexible molecules. In **1**, **2**, and **3·H₂O**, the symmetric ligand **L1** was always found to adopt a twisted endo−syn conformation despite demonstrating a variety of conformations in complexes using Ag(I) salts.[43] In **4·H₂O** and **5**, the unsymmetric ligand **L2** always opened out into an endo−anti arrangement. This conformational consistency may have arisen from the restrictions associated with binding to pseudo-octahedral metal centers. Although **3·H₂O** had a 2:1 metal-to-ligand ratio, the Cd(II) ion not involved in propagating the chain was present only as a side arm decoration. Thus, **3·H₂O** was closely related to the other four polymers which all had 1:1 metal-to-ligand ratios. The ligand **L1** was arranged in a head-to-tail fashion along the chains of **1** and **3·H₂O** except for a slight wagging of the rings in **1**. This resulted in U-shaped π-pockets which in both cases were occupied by anions. Unusually, these anions were involved in two different types of sandwich interactions, namely, π−anion−π and anion−π−anion (Figure 1). In **2**, ligands were also arranged in a head-to-tail fashion but alternate ligands were rotated by 150° about the axis of the chain creating a wider π-pocket segregated by a coordinated NO_3^- anion. The pocket contained three of the four anion−π interactions observed in **2** and the chains were interdigitated through complementary T-shaped π-interactions. It is conceivable in **1**, **2**, and **3·H₂O** that these anion−π interactions were responsible for templating the formation of the π-pockets. The polymer chains in **4·H₂O** and **5** were very similar to each other, except that in **5** coordinated NO_3^- anions occupied the axial positions in place of H_2O ligands. The benzene rings in **L2** which folded outward precluded the formation of π-pockets and instead were interdigitated with adjacent chains (Figures 11, 14). As a consequence of the ligand arrangement, the anions in both structures were involved in only anion−π−anion sandwich interactions. In **4·H₂O**, the ClO_4^- anions interacted with only one chain (Figure 10) while in **5** the coordinated NO_3^- anions acted as anion−π supramolecular synthons between chains (Figure 13).

Conclusion

It is interesting to speculate as to why these anion−π interactions appear to be so prevalent in this series of 1-D polymers of Co(II), Ni(II), and Cd(II) compared to coordination polymers of Ag(I) containing similar anions and ligands. Although anion−π interactions have recently been identified in Ag(I) complexes, those complexes involved very π-acidic ligand systems. In our systems, it seems that the conjunction of many factors has provided an environment favorable to

(43) Amoore. J. J. M.; Hanton, L. R.; Spicer, M. D. *Supramol. Chem.* **2005**, *17*, 557−565.

anion−π formation. First, the metals used have 2+ oxidation states and are generally stronger Lewis acids than Ag(I). When pyrazine is used to bridge these metal ions, a more π-acidic ring center is formed. Second, the ligand design can control the degree of anion−π interaction. The way in which the flexible ligand **L1** folds about an octahedral metal center places several π-acidic centers in close proximity to each other, thereby creating a cavity capable of interacting with anions. In principle, such cavities should provide better anion recognition by allowing for multiple interactions. In contrast, **L2** was designed to have just one π-acidic center to probe anion preference for different π centers. Consequently, these systems showed fewer types of anion−π binding while still maintaining an ability to interact with anions. This indicates that the polarizing effect of the metal ion is particularly important in anion binding when using less π-acidic heterocyclic rings such as pyrazine. A measure of how π-acidic these centers can become is evidenced by the previously unidentified complementary T-shaped pyrazine−π interactions observed in polymer **2**. Finally, the nature of the anion has consequences for the extended structure. For example, we have demonstrated that a coordinated anion has the ability to link neutral chains together via anion−π interactions and so provides a useful supramolecular synthon for self-assembly processes.

Our experimental investigation of the role of anion−π interactions in coordination−polymer chemistry gives credence to the concept of anion−π interactions as another type of important supramolecular interaction. This interaction has been found to be versatile and may have applications for the design of anion receptors and related host−guest systems.

Acknowledgment. We thank Professor Ward T. Robinson and Dr. Jan Wikaira (University of Canterbury) for X-ray data collection and the University of Otago Research Committee and the Department of Chemistry, University of Otago for financial support.

Supporting Information Available: X-ray data in CIF format. This material is available free of charge via the Internet at http://pubs.acs.org.

IC070194K